How RNA Unfolds and Refolds

Pan T.X. Li,[1] Jeffrey Vieregg,[2] and Ignacio Tinoco, Jr.[3]

[1]Department of Biological Sciences, University at Albany, State University of New York, Albany, New York 12222; email: panli@albany.edu

[2]Department of Physics, [3]Department of Chemistry, University of California, Berkeley, California 94720; email: jvieregg@berkeley.edu, intinoco@lbl.gov

Annu. Rev. Biochem. 2008. 77:77–100

The *Annual Review of Biochemistry* is online at biochem.annualreviews.org

This article's doi:
10.1146/annurev.biochem.77.061206.174353

0066-4154/08/0707-0077$20.00

Key Words

RNA folding kinetics, single molecule, force unfolding, FRET, helicase, translation

Abstract

Understanding how RNA folds and what causes it to unfold has become more important as knowledge of the diverse functions of RNA has increased. Here we review the contributions of single-molecule experiments to providing answers to questions such as: How much energy is required to unfold a secondary or tertiary structure? How fast is the process? How do helicases unwind double helices? Are the unwinding activities of RNA-dependent RNA polymerases and of ribosomes different from other helicases? We discuss the use of optical tweezers to monitor the unfolding activities of helicases, polymerases, and ribosomes, and to apply force to unfold RNAs directly. We also review the applications of fluorescence and fluorescence resonance energy transfer to measure RNA dynamics.

Contents

INTRODUCTION 78
SECONDARY STRUCTURE FOLDING 78
TERTIARY STRUCTRURE FOLDING 81
SINGLE MOLECULE STUDIES OF RNA ENZYMES 83
SALT EFFECTS ON MECHANICAL UNFOLDING OF RNA 85
Advantages of Mechanical Unfolding 85
Cation Binding in Mechanical Unfolding 86
Salt Effects on Secondary Structures 86
Salt Effects on Tertiary Structure .. 87
LIGAND AND PROTEIN BINDING TO RNA 88
ENZYMES THAT UNFOLD RNA 89
HELICASES 90
RNA-DEPENDENT RNA POLYMERASES 91
RIBOSOME 92
Translation 92
Mechanism of Elongation 92
SINGLE-MOLECULE TRANSLATION 93

INTRODUCTION

In 1999 one of us wrote a review article entitled "How RNA Folds" (1), which describes the RNA folding problem and contrasts it with the much more difficult protein folding problem. Atomic force microscopy was considered as a potential method to unfold RNA in physiological conditions of temperature and solvent; neither high temperatures nor denaturants would be needed. Since then laser (or optical) tweezers have emerged as the preferred method to apply force to unfold single molecules of RNA, because the technique allows direct observation of their unfolding and refolding. As an RNA molecule unfolds from tertiary structures to secondary structures to single strands (and refolds in reverse order), force and end-to-end distance of the RNA are measured; changes in the extension of the molecule indicate structural transitions in the RNA. Combining the force and distance measurements provides the work necessary to unfold the RNA, and the work obtained when the RNA refolds. If the process is reversible, the work done (or obtained) is the Gibbs free energy change. Kinetics are determined from the time dependence of the processes. A molecule that exists in two conformations can hop back and forth between the two states at equilibrium; the mean lifetime in each state and their distributions characterize the kinetics. Also, the force can be quickly jumped or dropped to a new value, and the lifetime of a conformation at the new value measured. Furthermore, measurements of fluorescence resonance energy transfer (FRET) on single molecules have revealed details of the kinetics of RNA folding and conformational changes.

In biological cells helicases exist to unwind specific RNAs; other enzymes, such as RNA-dependent RNA polymerases (RdRps) and ribosomes, need to unwind the RNA before they can perform their biological functions—transcribe or translate the sequence.

We summarize recent progress in unfolding RNA by force and by enzymes. We also discuss the application of single-molecule FRET to obtain novel kinetic and structural information about RNA reactions. Finally, we speculate about the contributions of single-molecule methods in the future.

SECONDARY STRUCTURE FOLDING

Experimental investigations of RNA secondary structure have been constrained by the stability of the folded state. With as few as three base pairs sufficient for duplex stability at room temperature, larger structures require high temperatures and/or chemical

denaturants to unfold. However, thermal melting data of secondary structure have been interpreted by a nearest-neighbor model (2) and form the basis for widely used structure prediction algorithms that predict secondary structure with reasonable accuracy (3–5). Using optical tweezers, an RNA structure can be unfolded into an extended single strand by mechanical force in physiological buffers and temperatures; structural transitions are indicated by changes in the extension of the molecule (6). Several RNA and DNA hairpins, derived from ribozyme, viral, ribosomal, and siRNA sequences (6–11), have been studied using this approach. Correction for the effect of force on the unfolded single strand is required, but this is measurable and can be also modeled (12). Recent investigations have also examined single-stranded homopolymers (13, 14). In addition, atomic force microscopy has been employed to examine the dissociation of RNA duplexes (15).

Force can be applied in several ways to study unfolding and refolding of single RNA molecules (9) (**Figure 1*a***). Increasing or decreasing the force at a constant rate (force ramp) generates a force-extension (F-X) curve (analogous to the pressure-volume curve for a gas) that characterizes the RNA's mechanical behavior (**Figure 1*b***). If the folding/unfolding transitions are assumed to be two-state transitions, it is possible to measure the rates from the resulting distribution of transition forces (16). Integration of the F-X curve yields the mechanical work done during the process; for a reversible process the mechanical work equals the Gibbs free energy change. Typically, the molecule does not unfold reversibly, which results in hysteresis in the F-X curve. Recent developments in nonequilibrium statistical mechanics, the Jarzynski (17) and Crooks relations (18), enable recovery of the reversible work, and thus the zero-force free energy of folding, from nonequilibrium experimental data (8, 19). Of these, the Crooks Fluctuation Theorem is particularly useful, as it is unbiased and converges more rapidly. Using this method, the effect (10 kcal mol^{-1}) of a single mutation on the folding free energy of the S15 three-helix junction was recovered (8). Theoretical investigations (20, 21) indicate that it should be possible to recover the complete free energy landscape along the force axis using this technique, even for folding that occurs away from equilibrium. This provides valuable information for understanding folding, but it remains to be seen whether experimental limitations make this technique possible in practice.

To directly measure the kinetics of unfolding or refolding, it is convenient to hold the force constant and measure the lifetimes of the folded or unfolded states (**Figure 1*c***). The rates $k(F)$ can be described by the following equation, (T: temperature in Kelvin, k: Boltzmann's constant):

$$k(F) = k_0 e^{\frac{FX^{\ddagger}}{kT}}. \qquad 1.$$

The derivative of $\ln(k)$ versus force yields the distance to the transition state $X^{\ddagger}$ for the folding or unfolding reaction. The pre-exponential k_0 is the apparent rate constant at zero force, but it cannot be compared with zero force kinetics measured by other methods, because the mechanism of unfolding or refolding will be different (6, 23, 24). Some hairpins unfold and refold rapidly near their equilibrium force. If many unfolding and refolding transitions are observed, the folding free energy landscape can be deconvolved from the probability distribution function of the extension of the molecule at a constant force, as demonstrated for several DNA hairpins (10, 11). This technique requires both a rapidly hopping molecule and a very stable instrument as many thousands of transitions must be observed to adequately sample rarely occupied areas of the potential. More often RNA molecules, especially those containing tertiary structure, have slow kinetics at their equilibrium forces. We have developed a force-jump technique (9) to rapidly change force between values such that folding and unfolding rates can be measured separately at different forces (**Figure 1*d***).

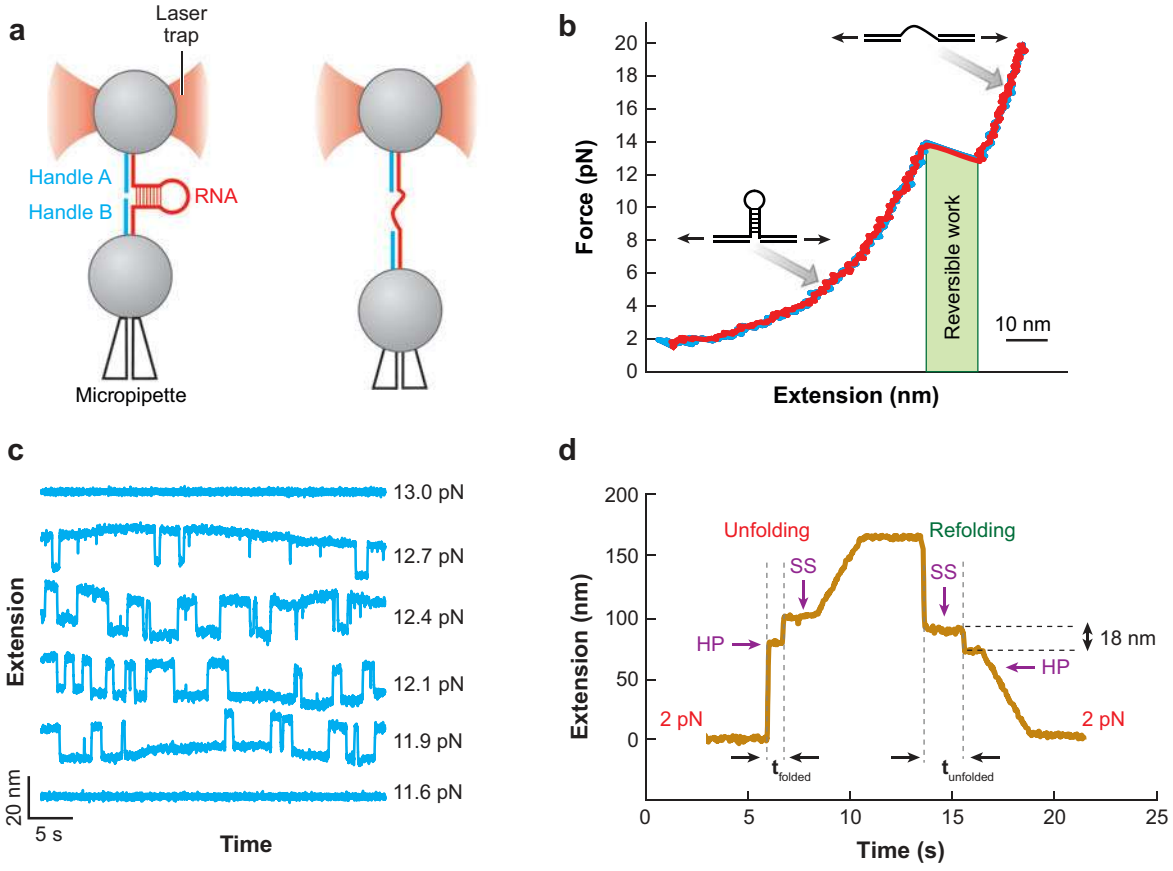

Figure 1

Mechanical unfolding of a hairpin. (*a*) A single RNA molecule consisting of a hairpin flanked by double-stranded DNA/RNA handles is tethered between two micron-size beads. One bead is held by an optical trap and the other is mounted on the tip of a micropipette. By moving the micropipette, the RNA is stretched and relaxed (22). (*b*) Force-extension curve of a pulling (*blue*) and relaxation (*red*) cycle. Un/refolding of the hairpin is characterized by a "rip" on the curve displaying negative slope. When the process is reversible, the area under the rip equals the un/refolding free energy. (*c*) When force is held constant near the equilibrium force, the extension of the molecule switches between two values corresponding to the folded and unfolded states. The lifetimes of the two states are force dependent. (*d*) Extension traces of a force-jump experiment. Unfolding and refolding kinetics of a hairpin can be monitored at different forces. Observations of lifetimes of folded and unfolded structures are collected to compute unfolding and refolding kinetics, respectively.

RNA can adopt alternative conformations with similar stability, and misfolding is a common phenomenon for RNA (25, 26). To reach the functional fold, the RNA must discriminate against nonnative conformations, some of which may be nearly as stable as the native state. The mechanism of this conformational search remains unclear. To understand the rugged folding energy landscape of RNA, it is indispensable to characterize alternative structures and their folding pathways. By varying the rate of force relaxation, the HIV-1 TAR sequence was steered to fold into the native hairpin in either one step or through multiple intermediates (27). When the force was relaxed quickly, the RNA misfolded, forming conformations with longer end-to-end extensions and decreased

stability relative to the native state. When force was increased subsequently, the RNA refolded into the native fold after the nonnative interactions were disrupted. Single-molecule manipulations, in combination with modeling of the folding pathways and intermediates (23, 24, 28–32), provide new opportunities to explore the energy landscape of RNA folding.

TERTIARY STRUCTRURE FOLDING

Tertiary interactions between distal domains are responsible for forming the compact three-dimensional structures required for many of RNA's catalytic and regulatory functions. Unfortunately, the predictive thermodynamic models that exist for secondary structure have not, to this point, been developed for tertiary structure. Whether such a model can be developed is one of the pressing questions for the RNA folding field. Many tertiary interactions are sufficiently weak that they can be disrupted using temperatures or solutions not too far from physiological conditions. The combination of clear comparison with function and greater accessibility has resulted in a much larger number of single-molecule studies of tertiary folding compared to secondary structure, especially by fluorescence techniques.

The majority of single-molecule investigations of tertiary folding have utilized the FRET technique [reviewed by Ha (34)] to monitor the distance between two dye-labeled nucleotides. This allows observation of the formation and dissociation of specific tertiary motifs in real time, a capability that complements the data obtained by force techniques. In addition to distinguishing discrete states (folded versus unfolded versus intermediates), the FRET signal quantitatively measures the distance between the labeled nucleotides. The FRET signals, though complicated by the need to account for variations in fluorophore characteristics and orientation, provide valuable constraints for structural modeling. Ha et al. (33) first demonstrated the utility of FRET for studying RNA folding by measuring conformational changes in a three-helix junction upon binding of Mg^{2+} or of a ribosomal protein. Subsequent experiments can generally be divided into two types: those which explore the folding of a specific RNA molecule (typically an enzyme) in detail, and those which primarily aim to investigate the folding dynamics of specific tertiary motifs. In this section, we focus on the latter, postponing discussion of ribozymes and ligand-binding RNAs for later sections.

One important motif that has been studied in this manner is the tetraloop-receptor interaction, in which a 4-nt hairpin loop (GNRA motif) docks with an asymmetric internal loop elsewhere in the molecule. This motif is present in many large folded RNAs and has been studied extensively by both structural and biochemical means (35). Tetraloop-receptor interactions have also been used to construct nanoscale synthetic RNA "building blocks" (36). A single-molecule FRET study (37) measured kinetics and equilibrium for docking of a GAAA tetraloop for an RNA in which the hairpin and receptor-containing duplex were linked by a short strand of polyA (**Figure 2*a***). The docking rate increased 12-fold as the concentration of Mg^{2+} was increased from 0 to10 mM (**Figure 2*b***), consistent with observations in bulk studies. The undocking rate was found to decrease by a factor of three over the same range of Mg^{2+} concentration. A follow-on study explored the effect of changing the linker sequence and/or length (38), concluding that the linker acted solely to increase the effective concentration of the loop and receptor and did not change the equilibrium constant. In these studies, considerable heterogeneity was observed in molecular behavior, both kinetically and in the equilibrium species present. Such heterogeneity would complicate data interpretation in bulk studies.

When single-molecule measurements are combined with traditional molecular biology

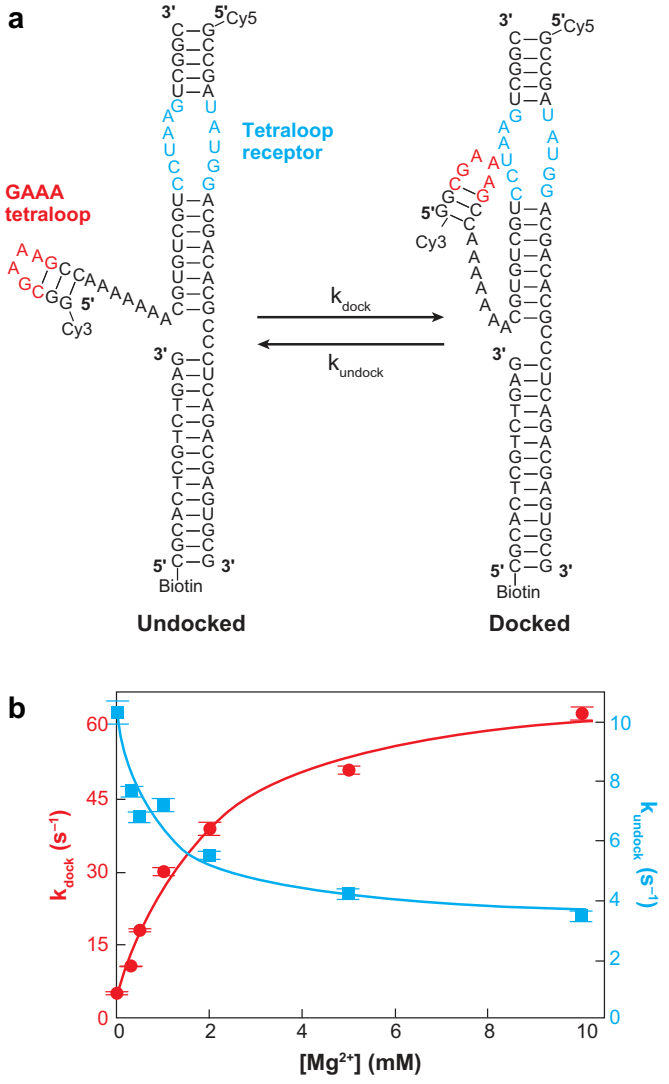

Figure 2

Single-molecule measurement of a tetraloop-receptor tertiary interaction. (*a*) Three strands of RNA were annealed to form a duplex that contains the receptor (*blue text*) linked to a short hairpin containing a GAAA tetraloop (*red*) by a flexible $(A)_7$ tether. Fluorophores Cy3 and Cy5 were placed at the ends of the hairpin and duplex, resulting in fluorescence resonance energy transfer (FRET) efficiencies of 0.68 and 0.22 for the docked and undocked states, respectively. (*b*) Docking and undocking kinetics as a function of [Mg^{2+}]. Adapted from Reference 37.

techniques such as mutagenesis, it is possible to understand folding processes in even more detail, as demonstrated in a study of the duplex docking interaction that forms the core of the *Tetrahymena* ribozyme (39). The P1 duplex is a five-base-pair helix which, when docked, forms a minor groove triplex with two single-strand sections of the ribozyme core. Both the duplex and its docking target are preformed. The docking dynamics were measured by a FRET signal of fluorophores on the duplex and the receptor. All 8 nts of P1 that make tertiary contacts were successively mutated and the docking and undocking rates were measured. Each mutation caused a significant change in the equilibrium constant of the reaction. Surprisingly, the docking rate was largely unaffected by addition of urea or mutations, suggesting that the transition state for docking does not resemble the docked state. Together with bulk chemical protection data (40), these results suggest that the rate-limiting step of duplex docking may be escape from a kinetic trap, possibly a misfolded structure of the J8/7 docking target. Recent reseach finds that combining cyclic repeated Mg^{2+} jumps with single-molecule FRET reveals slow degrees of freedom in folding of the catalytic domain of RNase P that were not apparent from typical salt-jump experiments (Xiaohui Qu, personal communication). Both of these studies illustrate the power of combining single-molecule techniques with traditional biochemical methods to reveal features inaccessible to either alone.

A kissing interaction is the base pairing formed by complementary sequences between two hairpin loops (41). Using optical tweezers, we studied an intramolecular kissing complex formed by two hairpins linked by A_{30}; this minimal kissing complex contains only two G·C base pairs (42). By increasing force, the RNA was unfolded into four different conformations in order: kissing complex, two linked hairpins, one hairpin, and single strand. As force is decreased, the single strand was refolded into the kissing complex in the reverse order. Kinetics of steps in the unfolding and refolding were measured. In contrast to the hairpins the unfolding rate for the kissing interaction was found to be relatively insensitive to force. The distance to the transition state for breaking the kissing interaction

($X^{\ddagger} = 0.7$ nm) indicates that both kissing base pairs were broken at the transition state. The kissing loop was also found to lock the two hairpins in place at forces significantly higher than those required to unfold the hairpins alone. This phenomenon is likely due to the orientation of the kissed hairpins relative to the force axis (42).

Pseudoknots, also a common motif in RNA structure, are critical in programmed ribosomal frameshifting (43), telomere structure (44), and ribozyme activity (45). Folding free energies of various pseudoknots have been measured in bulk (43). A substantial effort is underway to codify their thermodynamics and kinetics in an analogous manner to the nearest-neighbor model of secondary structure (46–49). Experimentally, two groups have used optical tweezers to investigate pseudoknot folding at the single molecule level. Hansen et al. measured the force required to unfold two molecules patterned after the infectious bronchitis virus (IBV) frameshifting pseudoknot (50). Independently, we also studied the mechanical unfolding of the wild-type IBV pseudoknot and two mutants as well as the constituent hairpins (51). The folding kinetics and free energies for these molecules were measured. Together, these measurements cover a variety of different stem lengths and nucleotide compositions, which should be helpful in constructing a more accurate picture of the energy landscape and folding pathway for this important tertiary interaction.

The primary challenge in understanding RNA tertiary structure is to uncover the general principles that govern its folding and dynamics. However, a rigorous folding algorithm for prediction of tertiary structure is not yet available (52). Single-molecule studies, together with more ensemble measurements, can provide important constraints to be utilized in computation and to serve as test cases for modeling. Moreover, most functions of RNAs, such as catalytic activities, depend on the dynamics of the molecules. In proteins, molecular dynamics (MD) simulation has been extensively employed to explain observation of single-molecule dynamics at the atomic level (53). Similar work in RNA is lamentably rare. One exception is a recent paper by Rhodes et al. (54), in which MD simulation is used to model the water molecules trapped in the catalytic core of a ribozyme. The simulation predicted changes in hydrogen networking caused by specific mutations. A surprising linear correlation was found between the loss of water-mediated hydrogen bonds and the reduction of docking free energy relative to the wild-type enzyme. Collaboration between experimentalists and modelers at the design stage is particularly useful, as data and simulation can then inform each other synergistically rather than after the fact.

SINGLE MOLECULE STUDIES OF RNA ENZYMES

Ribozymes have been a preferred target for single-molecule studies of RNA for nearly as many years as the techniques have existed (55). FRET has been the preferred method, and folding is typically studied by adding Mg^{2+} ions to molecules with preformed secondary structure and observing the resultant conformational changes. Ribozyme folding, and single molecule studies thereof, were the subject of two recent reviews (56, 57). In this review, therefore, we focus on several recent results that may point the way toward future progress in the field.

The first generation of single-molecule ribozyme experiments mostly focused on the folding of the enzyme from secondary to tertiary structure. Although interesting as a study of RNA folding, these results do not directly bear on the main function of ribozymes, which is catalysis. Working with inactive enzymes avoids the problem of losing one's sample via self-cleavage, but makes it hard to determine the relationship between observed conformational dynamics and the catalytic cycle. Nahas et al. (58) were able to overcome this difficulty for the self-cleaving hairpin ribozyme by adding a single-strand RNA that resembled the cleavage product, but was extended with

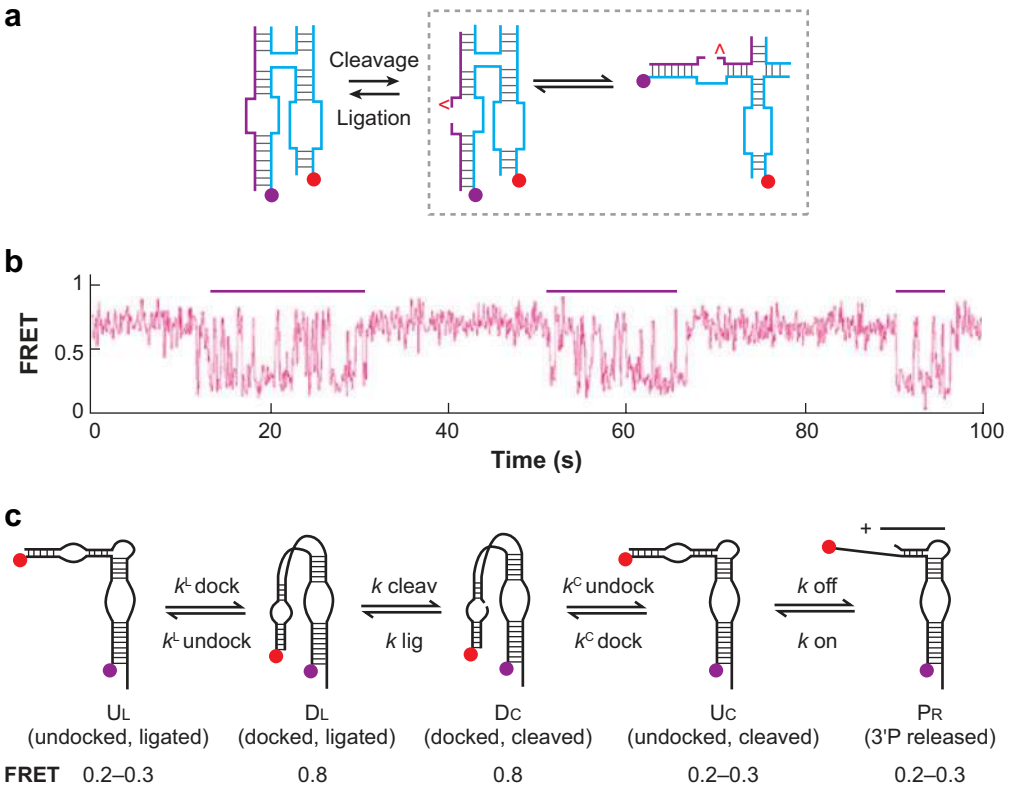

Figure 3

Observing active hairpin ribozymes with single molecule fluorescence resonance energy transfer (FRET). (*a*) Extended product strand (*purple*) remains bound after cleavage (site marked with ^), enabling a multiple turnover assay. (*b*) FRET trace of a single ribozyme undergoing multiple rounds of cleavage and ligation, as described in (*a*). The cleaved enzyme (*purple bars*) switches rapidly between two FRET values. The lower value represents the undocked state and the higher the docked state. The uncleaved RNA has a stable FRET efficiency of about 0.7. (*c*) Reaction mechanism of a variant hairpin ribozyme. States with similar FRET values can be distinguished by changing Mg^{2+} and product concentrations. Panels *a* and *b* adapted from (58) and *c* from (59).

nucleotides complementary to the ribozyme. Once the ribozyme cleaved itself, the new strand remained bound to the ribozyme and was religated by the reverse reaction. This approach, which can be applicable to other enzymes, enabled them to observe multiple cycles of cleavage and ligation (**Figure 3*a*,*b***). The researchers were able to correlate the docking/undocking with catalytic rates of the enzyme in a pH-dependent manner. Recently, Zhuang and coworkers reported an alternate scheme to dissect the reaction pathway of a variant of the hairpin ribozyme (59). A series of Mg^{2+} pulse-chase experiments were performed to identify kinetic "fingerprints" of the various enzymatic states (undocked, docked, docked and cleaved, cleaved and undocked, and product released, **Figure 3*c***) in a single enzymatic cycle. Different states with similar FRET signals, such as cleaved and uncleaved RNA at docked conformations, could be distinguished, revealing a detailed kinetic mechanism of the hairpin ribozyme.

Among the exciting discoveries in recent years is the expansion of the types of chemistry that RNA enzymes are capable of

performing. In addition to the naturally occurring phosphodiester cleavage/ligation reaction, in vitro selection approaches have revealed ribozymes that catalyze a diverse array of chemical processes, including oxidation/reduction, nucleotide synthesis, and peptide bond formation (60). This has added support for the "RNA World" hypothesis of biochemical origins (61). Although a fruitful tool for discovering new activities, in vitro selection is largely silent regarding the mechanism of the enzymes that are discovered. Single-molecule techniques, with their capability to resolve rare and short-lived intermediates, should be very valuable in determining how these new ribozymes work. A recent example of this is a study of the Diels-Alder ribozyme carried out by Kobitski et al. (62). Working with a truncated, but functional, form of the enzyme, they were able to observe that the enzyme undergoes interconversion between two states at equilibrium at a rate of $\sim 20\ s^{-1}$. This conformational switching appears to resolve a conflict between the solved crystal structure and bulk chemical assay results: The crystal structures indicated that the product was trapped in the active site. Future studies on this and other novel ribozymes should further increase our knowledge of the various chemistries that RNA can participate in, particularly if combined with functional assays and MD simulation.

SALT EFFECTS ON MECHANICAL UNFOLDING OF RNA

RNA is a polyelectrolyte with one negative charge per phosphate. Consequently, RNA depends critically on ionic conditions for its structure, stability, reactivity, and ability to bind to ligands and proteins. Like other polyelectrolytes, RNA attracts cations to form a conterion atmosphere around it. These closely associated cations show similar self-diffusion coefficients to the much larger polymer (63–65). However, RNA cannot be simply treated as a cylindrical polyelectrolyte with infinite length (66–71). RNAs have a wide variety of sizes and shapes; in addition to diffuse metal ion binding, RNA tertiary structure often contains specific binding sites for divalent metal ions like Mg^{2+}. Both diffuse and specific cation binding are critical for stability of RNA secondary and tertiary structures (72, 73), with tertiary structure particularly dependent on specific binding. Definitions of diffuse and specific binding are somewhat arbitrary; there is no clear boundary to distinguish the two types of binding. Cation binding to RNA is relatively weak; for instance, the K_d of specific Mg^{2+} binding is often in the millimolar range.

Salt effects on nucleic acids have been extensively studied and reviewed elsewhere (66–70, 74). Here, we discuss how mechanical unfolding techniques can be employed to probe some perennial problems in understanding salt effects on RNA structure and folding.

Advantages of Mechanical Unfolding

Mechanical unfolding offers several advantages over bulk methods in studying ion binding to RNA. First, force applied by optical tweezers (<150 pN) changes only the noncovalent interactions in the RNA. Unfolding, especially of secondary structure, can be studied at physiological temperatures regardless of ionic conditions. This is a big advantage over thermal denaturation, during which RNA degrades at high temperature, especially in the presence of Mg^{2+}. Second, thermodynamic interpretation of mechanical unfolding results is straightforward because locally applied force changes RNA structure, but not activities of ions and water molecules. Moreover, RNA is so dilute in single-molecule experiments that the reaction chamber is almost a solution of salt, thereby avoiding complicated treatment of colligative properties of concentrated RNA solutions (63). Third, development of force manipulation technique provides precise control of RNA conformations, allowing direct evaluation of disruption

or formation of a particular interaction (42). Hence, ionic effects on folding secondary and tertiary structures can be disentangled.

Cation Binding in Mechanical Unfolding

How is mechanical unfolding of RNA affected by force and ionic conditions? Here we describe a simple thermodynamic scheme for an unfolding reaction,

$$\text{Folded} + n_1 M \leftrightarrow \text{Unfolded} + n_2 M,$$

in which M refers to a metal ion; and n_1 and n_2 are numbers of metal ions associated with folded and unfolded conformations. The effect of salt on unfolding can be written as

$$\frac{\partial \ln K_{eq}}{\partial \ln [M]} = \Delta n, \qquad 2.$$

in which K_{eq} is the equilibrium constant (ratio of unfolded to folded conformation), $\Delta n = n_1 - n_2$ is the net change in metal ions in the unfolding, and $[M]$ is the total concentration of metal ions. We can describe the effect of metal ions on the mechanical unfolding of RNA as

$$\ln K_{eq,F} = F\Delta X/k_B T + \ln K_0 + \Delta n \ln[M], \qquad 3.$$

in which $K_{eq,F}$ is the equilibrium constant at force F, and K_0 is the apparent equilibrium constant extrapolated to zero force and zero salt. Equation 3 can be directly applied to RNA folding in a monovalent cation solution. However, RNA folding, particularly that of tertiary structure, is often studied by varying the concentration of Mg^{2+} ions while holding the monovalent concentration at a constant value of typically several hundred millimolar. In these conditions, the monovalent salt can be treated as part of the solvent; and the $\Delta n \ln[M]$ term can be used to describe the effect of Mg^{2+}. We note that ΔX (and $X^{\ddagger}$) depends on the force (75); when free energy and kinetics are extrapolated to forces far away from the transition forces, ΔX can vary significantly. It is possible that Δn also varies with force.

Salt not only affects the folded and unfolded states, but also the height of the kinetic barrier. Salt effects on thermodynamics and kinetics are usually parameterized by ΔG_{ionic} and $\Delta G^{\ddagger}_{ionic}$, respectively. For a two-state unfolding reaction with a single transition state (**Figure 4*a***), cations raise the height of the kinetic barrier but do not change the position of the transition state along the reaction coordinate for unfolding. On the ln k versus force plot, the slope of the curve ($X^{\ddagger}/k_B T$) is constant but the y-intercept decreases as cation concentration increases. The first-order un/refolding kinetics can be written as

$$\ln k = FX^{\ddagger}/k_B T + \ln k_0 + \Delta n^{\ddagger} \ln[M], \qquad 4.$$

in which k is the rate constant, k_0 is rate constant extrapolated to zero force and zero $[M]$, and $\Delta n^{\ddagger}$ reflects change in the number of cations bound to RNA at the transition state.

It is tempting to interpret Δn and $\Delta n^{\ddagger}$ as the effective numbers of salt bridges formed, or effective numbers of counterions released, upon RNA structural transitions or ligand binding. This simplified view does not take into account the effect of counterion condensation and shapes of RNA molecules, but more thermodynamically rigorous treatments for mono- and divalent metal ion bindings for RNA have been developed (76–79). However, Δn and $\Delta n^{\ddagger}$ can be conveniently used to describe the ionic effect on the un/refolding kinetics.

Salt Effects on Secondary Structures

The effect of Mg^{2+} on the stability of several RNA hairpins and a three-helix junction (6, 8) was studied. In general, RNA hairpins unfold and refold at higher forces as salt concentration increases; and Mg^{2+} shows a much stronger effect than monovalent cations. An example of such an effect on a TAR hairpin (P.T.X. Li, unpublished data) is shown in **Figure 4*b***. The critical force, $F_{1/2}$, at which unfolding and refolding rates are equal, increased by ~6.5 pN upon addition of 10 mM

Mg^{2+}, whereas ΔX of unfolding the hairpin changed less than 2 nm. We have varied concentrations of monovalent cations and concentration of Mg^{2+} up to 30 mM in the presence of 100 mM KCl. The reversible mechanical work required to unfold the hairpin and $\Delta G(0\ pN)_{22^\circ C}$ appears to increase linearly with the logarithm of concentration of cations. This linearity is consistent with bulk observations (80).

The stabilizing effect of metal ions on RNA hairpins results from both a decrease in the unfolding rate and an increase in the folding rate. $X^{\ddagger}$ of unfolding and refolding remained largely unchanged by type and concentration of cations, and $\Delta n^{\ddagger}$ appeared to be constant for each type of cation. Hence, Equations 3 and 4 are suitable for description of salt-dependent thermodynamics and kinetics of folding secondary structure.

Interestingly, metal ions have a stronger effect on unfolding than refolding (6, 8). In the F-X curves, hysteresis between the unfolding and refolding trajectories increases with salt concentration. This effect is also shown by reduced overlap between the unfolding and refolding force distributions at high salt conditions (**Figure 4*b***). The weaker salt dependence of refolding kinetics probably results from its reaction mechanism. The rate-limiting step of hairpin folding is formation of the loop-closing base pair, which must compete with alternative combinations of base pairs (80, 81). Cations facilitate this process by offsetting the negative charges on the phosphates but are unlikely to discriminate against nonnative base pairs.

Cations, particularly monovalent cations, bind diffusely to a simple hairpin. But Mg^{2+} displays specificity to bulges and internal loops and affects dynamics of their neighboring domains (82, 83). These unpaired regions in the RNA are also interesting because many of them bind small molecule ligands and can be used as drug targets, a process that requires displacement of counterions (84, 85). Salt effects on mechanical unfolding of these structures remain unexplored.

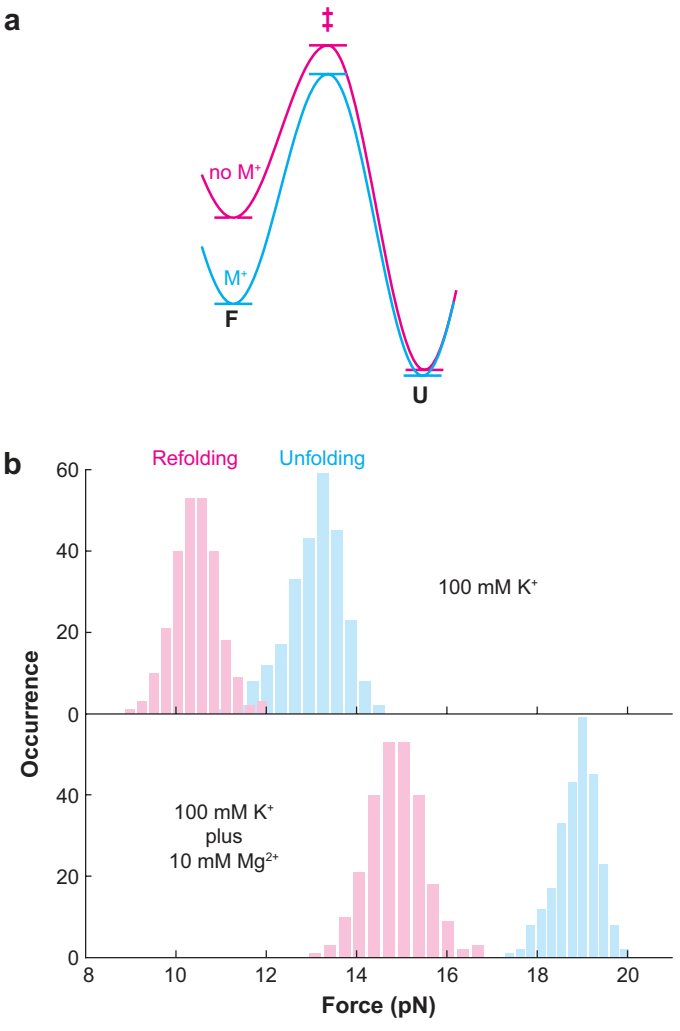

Figure 4

Salt effects on force unfolding of RNA structure. (*a*) Effect of a cation, M^+, on a simple two-state unfolding reaction. The cation stabilizes the folded structure, effectively raising the kinetic barrier for unfolding. Salt effects on the unfolded state are less than that on the folded state. The position of the transition state along the reaction coordinate is not affected by the cation. (*b*) Force distributions of TAR RNA in 100 mM KCl (*top*) and with an additional 10 mM Mg^{2+} (*bottom*) (P.T.X. Li, unpublished data).

Salt Effects on Tertiary Structure

Folding and stability of tertiary structure are critically dependent on ionic conditions, especially Mg^{2+}. Consequently, metal ions have more pronounced effects on tertiary structure than on secondary structure. Kinetics of breaking tertiary interactions are greatly

slowed by Mg^{2+}, but folding rates of tertiary structure are only moderately dependent on metal ions.

Intron ribozyme. The first hint of Mg^{2+} effects on mechanical unfolding of RNA tertiary structure came from a study by Onoa and colleagues (86). Mechanical unfolding of the L-21 ribozyme in 10 mM $MgCl_2$ was characterized by distinct rips, each of which represents unfolding of a structural domain. In the absence of Mg^{2+}, the RNA populated collapsed conformations as observed in bulk studies (87), and its unfolding trajectories showed no clear rips. As the concentration of Mg^{2+} was increased, unfolding rips gradually appeared at forces significantly higher than those required to disrupt the collapsed forms, indicating differential Mg^{2+} dependence of individual interactions and domains (supporting materials in Reference 86).

Pseudoknots. Pseudoknots adopt compact structures (43), and their stability depends on bound Mg^{2+} (73, 88). In one of the recent mechanical studies on pseudoknots (51), Mg^{2+} not only raised the rip force but also decreased $X_{unfolding}^{\ddagger}$, as evidenced by changes in the force-dependent unfolding rates.

Loop-loop interactions. Using force manipulation, formation and disruption of an intramolecular kissing complex can be directly observed and distinguished from un/refolding of secondary structures (42). The salt dependence of kissing interactions depends on the sequence of kissing base pairs. A well-studied case is two variants of the DIS kissing complexes derived from HIV-1, in which kissing sequences are GUGCAC (Mal) and GCGCGC (Lai) (41, 89, 90). Mg^{2+} has a strong stabilizing effect on both kissing complexes. Addition of 1 mM Mg^{2+} raised the mean rip force to break the kissing interaction by over 20 pN (P.T.X. Li, unpublished data). Yet, unfolding of the two kissing complexes displayed different force and salt dependences, as evidenced by different values of $X_{unfolding}^{\ddagger}$ and $\Delta n_{unfolding}^{\ddagger}$. Kinetics of breaking the kissing interactions can be well described by Equation 4.

Ongoing efforts to understand salt effects on RNA tertiary interactions by force unfolding can yield key thermodynamic and kinetic parameters. These new parameters need to be explained structurally. For instance, is $\Delta n_{Mg^{2+}}^{\ddagger}$ the number of Mg^{2+} released at the unfolding transition state? Are these Mg^{2+} ions bound to specific sites or diffusely associated with the RNA? Because unfolding kinetics directly reflect the folded RNA complexed with cations, unfolding kinetics may be more useful than the folding free energy in interpretation of cation binding.

LIGAND AND PROTEIN BINDING TO RNA

A DNA or RNA molecule can be mechanically unfolded in the absence and presence of ligands and proteins; differences in stability reflect the binding of ligands. A DNA helix can be mechanically perturbed either by shearing (pulling on opposite ends of the helix) or by unzipping (pulling the two strands apart from the same end of the helix). In the shearing mode, ligand and protein binding are indicated by global changes in the molecule's F-X curve (91); the binding affinity at both zero force and high forces can be quantified (92). For the unzipping experiments, displacement of specifically bound proteins results in a clear rip (abrupt change in extension) when the unfolding fork displaces a bound protein (93–95). This approach can be used to map the protein binding site along the DNA duplex. Applying this strategy to RNA, we found that argininamide, but not arginine, binds and stabilizes the TAR hairpin, confirming the specificity of argininamide for this RNA (96). We expect to see more mechanical studies on ligand- and protein-RNA interactions in the near future.

Single-molecule fluorescence techniques have demonstrated great potential in studying assembly and dynamics of large

ribonucleoproteins (RNP). Because many extensive reviews are available (57, 97), we only briefly introduce three very recent studies. A straightforward but especially important application of single-molecule fluorescence techniques is counting the numbers of subunits in an RNP, an often difficult task for a large multicomponent complex. For instance, it has been deduced from electron cryomicroscopy and crystallography (98) that each bacteriophage phi29 DNA-packaging motor has six packaging RNA (pRNA) molecules. In a recent experiment (99), pRNAs, each labeled with a fluorophore, were incorporated into the packaging motor. By sequentially photobleaching fluorophores on single motors, stoichiometry of six pRNA per motor has been confirmed.

Annealing of two hairpins with complementary sequences into a duplex requires unfolding of both hairpins. In HIV, TAR RNA is annealed to its complementary DNA (cTAR) sequence with the help of the nucleocapsid protein during the critical minus-strand transfer step (100). The role of the protein in this process remains unclear. Combining microfluidic techniques with single-molecule FRET and fluorescence correlation spectroscopy, Barbara and colleagues observed many intermediates in the annealing of TAR and cTAR, revealing both the annealing pathway and the chaperone activity of the nucleocapsid protein (101, 102).

Assembly of RNPs is often sequential, suggesting that early protein binding events induce a conformational change in RNA that allows subsequent associations. By labeling a pair of fluorophores at various positions of the telomeric RNA, Stone and colleagues have demonstrated that binding of p65 protein induces a conformational change in the telomere RNA that facilitates the binding of the telomerase reverse transcriptase (103).

ENZYMES THAT UNFOLD RNA

In physiological conditions RNA folds spontaneously, but requires energy to unfold. A single base pair closing a loop in RNA is not stable, because base-base hydrogen bonds are only slightly more stable than base-water hydrogen bonds, and there is a loss of entropy on constraining the RNA to form a loop. The free energy change is positive. However, adding successive base pairs soon produces a stable structure with a negative free energy change relative to the single strand. At 37°C three G·Cs closing a tetraloop (GCG[UUCG]CGC) are stable by –2.4 kcal mol^{-1} in 1 M NaCl; it takes five A·Us (AUAUA[UUCG]UAUAU) to become stable with a $\Delta G = -1.9$ kcal mol^{-1} (104). Each additional base pair—depending on the sequence—decreases the free energy by –1.0 to –3.4 kcal mol^{-1}. In ionic environments more closely resembling those of a cell (100 mM univalent, 10 mM divalent ions), the free energies are expected to be similar. The standard free energy of hydrolysis of ATP at 37°C is –7.4 kcal mol^{-1}, therefore the cell must burn one ATP to unfold three to four RNA base pairs. An alternative way to unfold RNA is to bind the single strand by a single-strand specific protein. The binding to the single strand must be strong enough so that it can compete with base pair formation. An average ΔG of +2 kcal mol^{-1} for breaking a base pair means that the dissociation constant for single-strand specific protein is increased by a factor of 25 ($e^{\Delta G/RT}$) for each base pair that is broken before binding can occur. Thus, if four base pairs must be unfolded to form a single-strand binding site for a protein, the dissociation constant for binding the single strand increases by two orders of magnitude.

RNA must be single stranded for its sequence to be interpreted during viral RNA replication and translation, so it must first be unfolded by the RNA-dependent RNA polymerase or ribosome, or by a helicase that assists the unfolding. The enzymes use the chemical energy available in the hydrolysis of nucleoside triphosphates to unfold their RNA substrates. The functions of these molecular motors require them to work on RNAs of

widely differing sequences. They are promiscuous; however, initiation of their activity often involves specific sequences and structures.

HELICASES

Helicases are molecular motors that convert the chemical energy of ATP hydrolysis into removing bound proteins and mechanically separating the strands of double-stranded nucleic acids (105). The DEAD-box family of RNA helicases belongs to protein superfamily II and is by far the largest family of RNA helicases—over 500 sequences are known (106). Several crystal structures have been published, including the structure of the NS3 hepatitis C helicase bound to DNA (107), and the structure of a thermophilic RNA helicase bound to ATP (108). The many biochemical functions of helicases have been reviewed (106, 109, 110). We concentrate on their mechanism of action, particularly by single-molecule studies (111).

Two RNA helicases essential for viral replication have been extensively studied: NPH-II helicase from vaccinia virus (112, 113), and NS3 helicase from hepatitis C virus (114–117). Both load on an overhanging 3′-single strand and move in a 3′-to-5′ direction. Unwinding begins when the helicase arrives at the junction of the double strand and single strand; the helicase then unwinds the RNA in a series of bursts and pauses. During the pause the helicase can dissociate from the RNA or begin another step of unwinding. The number and size of unwinding steps that occurs determines the processivity of the process (118). The fundamental characteristics of these helicases (step sizes, efficiency, processivity) are not well established. It is not even certain how many helicases are actually working on each RNA in different experiments.

Single-molecule studies of the hepatitis C virus RNA helicase were done by attaching the ends of an RNA containing a hairpin to two beads and monitoring the increase in end-to-end distance of the RNA as a helicase unfolded the molecule at constant force (116). The extension versus time showed discrete unwinding steps (extension increased with time) followed by pauses (extension did not change during the pause). The translocation steps were 11 bp with substeps of 3 to 4 bp, independent of ATP concentration. This result contrasts with an earlier ensemble experiment, which found an average step size of 18 bp (114). The difference in measured step size between single-molecule and ensemble experiments were attributed to differences in the oligomeric state of the active helicase; monomeric in the former and dimeric in the latter. However, in neither experiment was the actual number of RNA-bound helicases measured.

The single-molecule experiments allowed measurement of the effects of experimental variables (ATP, RNA sequence, force) on each step in the helicase mechanism. Increasing ATP concentration increases the rate of reaction, as expected, but has no effect on processivity. Increasing ATP concentration decreases both the length of each pause and the time for each unwinding step. Analysis of the dependence of the pauses, unwinding steps and substeps on ATP concentration indicates that at least one ATP is involved in each pause and substep. The unfolding of 11 bp clearly requires more than one ATP to be hydrolyzed per cycle of pause and translocation.

Single-molecule fluorescence studies (119) of the hepatitis C NS3 helicase unwinding DNA have found steps of 3–4 bp, with evidence of 1-bp substeps and 1 ATP hydrolyzed per base pair. How much of the differences is due to DNA versus RNA substrates or other differences in the experiments (such as force assistance) requires more work.

A question that is often posed for molecular motors is whether they take advantage of thermal energy to move—are they passive motors or do they actively destabilize base pairs (120)? To test whether the HCV helicase acts like a passive Brownian motor that waits for the double-stranded region to open spontaneously before moving forward, the

kinetics were compared with the probability of thermal base-pair opening of different RNA sequences. Two 60-bp hairpins were studied; one contained 30 A·Us followed by 30 G·Cs; the other had the two sequences interchanged so that the NS3 helicase encountered the G·Cs first (117). The kinetics of unwinding a helix by a pure Brownian mechanism should vary with $e^{-\Delta G^\circ/RT}$, the exponential of the free energy of base pair opening (ΔG°) compared to thermal energy, RT. At 37°C, ΔG° for opening a single base pair in the sequence $\frac{AA}{UU}$ is 1.0 kcal mol^{-1}, it is 3.3 kcal mol^{-1} for opening a base pair in the sequence $\frac{GG}{CC}$ (104). The difference in free energy corresponds to a 42-fold faster rate for passive opening of one base pair at a time from the A·U sequence compared to the G·C sequence. If the helicase opens two base pairs at a time, the calculated rate increase for A·Us over G·Cs becomes 1750. The observed rates of helix unwinding changed much less with sequence. NS3 pauses 10 times longer and translocates 3 times slower on G·C base pairs than A·U base pairs. This result shows that the HCV helicase is not a passive Brownian motor, but actively opens base pairs. A ring-shaped helicase from T7 that unwinds DNA has also been found to be an active motor (121).

The processivity of NS3 also depends on the G·C content; strong barriers accelerate NS3 detachment from RNA before the base pairs are unwound. The probability that the helicase dissociates from the RNA increases as it approaches a G·C sequence; this increase occurs up to 6 bp ahead of the opening fork (117).

Force applied to the hairpin changed neither the helicase's step size, nor its rate of unwinding. However, increasing force did increase processivity. This implies that force destabilizes the double strand, decreasing the barrier to unfolding and favoring the enzyme remaining bound to the RNA during pauses.

A mechanistic picture consistent with all these results (116, 117) is that the helicase has one site that binds the single-stranded RNA and another that binds and destabilizes the double-stranded RNA ahead of the unwinding fork. The single-strand binding site inches forward unwinding base pairs until it reaches the double-strand binding site. The double-strand binding site releases the RNA, the helicase stretches, and the site binds and destabilizes the RNA duplex ahead to repeat the cycle (**Figure 5**). The probability that the helicase will release from the RNA, and thus decrease the processivity, depends on the stability of the helix. A helix with high G·C content will decrease binding and destabilization of the duplex by the double-strand binding domain and may allow the single-strand site to release the helicase. Force on the hairpin will destabilize the helix and thus increase the processivity.

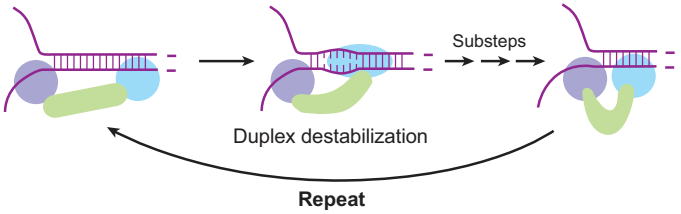

Figure 5

An inch worm model of the motion of NS3 helicase adapted from Reference 116. In each translocation step, the helicase reaches ahead and destabilizes the double strand; the single-strand binding site then inches forward unwinding the duplex.

RNA-DEPENDENT RNA POLYMERASES

RNA viruses—other than retroviruses—are replicated by their viral-encoded RdRps. These polymerases must synthesize both plus strand and minus strand chains. They can initiate from primers or by de novo initiation usually starting with a GTP. Non-viral RdRps also exist in many organisms. They synthesize RNAs from RNA templates and are involved in many cellular functions, including RNA silencing (122).

Although many single-molecule studies of DNA-dependent RNA polymerases (DdRps) have been done (123–126), RdRp studies have

not yet appeared. The experiment could be exactly analogous to the helicase study described here, or follow the DdRp-type experiments. There the enzyme is attached to one bead and the distance between the enzyme and 5′ end of the RNA is monitored.

RIBOSOME

The ribosome is a very complex molecular machine that catalyzes the hydrolysis of GTP to translate messenger RNAs into polypeptides (127, 128). High resolution structures are only available for prokaryotic ribosomes, and single-molecule experiments have not been done on eukaryotic ribosomes, therefore we limit ourselves here to the prokaryotes. The function of ribosomes is so important to life that it is the objective of many researchers to establish a detailed motion picture of the action of a ribosome during translation. The goal is a mechanism of translation that characterizes the conformation of the ribosome and the positions of the mRNA, the tRNAs, and the translation factors at each step in the process. The energy at each step, and the barriers between steps—the thermodynamics and kinetics of the process—are also necessary to understand the operation of the ribosome. We summarize the progress here with emphasis on single-molecule studies of the motion of the mRNA and tRNAs.

Translation

Initiation occurs with the binding of an mRNA, formyl methionine tRNA (fMet-tRNA^{fMet}), and initiation factors IF1, IF2·GTP, and IF3 to the 30S subunit of the ribosome. Next the 50S subunit is recruited, GTP is hydrolyzed, and the initiation factors are released, leaving the fMet-tRNA^{fMet} bound at the P-site of the ribosome. Elongation starts when EF-Tu·tRNA·GTP binds to the ribosome, which has a peptidyl-tRNA or fMet-tRNA in the P-site. Interaction of the EF-Tu with the ribosome catalyzes the hydrolysis of the GTP, the correct aminoacylated-tRNA is left at the A-site, and EF-Tu·GDP is released. A new peptide bond is formed when the α-amino group of the A-site amino acid attacks the carboxyl carbon of the amino acid linked to the P-site tRNA. As a peptide bond replaces an ester linkage, this step in the the reaction is spontaneous, and free energy decreases. Once the peptide chain has been transferred to the A-site tRNA, a hybrid state is favored in which the 3′ end of the P-site tRNA moves to the exit site (E-site) and the 3′ end of the A-site tRNA moves to the P-site. Now EF-G·GTP binds and translocation occurs as GTP is hydrolyzed by interaction with the ribosome. Translocation involves the movement of the mRNA with the two tRNAs by 3 nts to position the next codon at the A-site of the 30S subunit. Translocation can occur even in the absence of EF-G, but it is very slow. Translation stops when a stop codon is reached. A release factor recognizes the stop codon and hydrolyzes the completed polypeptide from the P-site RNA.

During translation the ribosome must be able to process 61 different codons and 3 different stop signals. It interacts with a minimum of 20 tRNAs, but it can interact with up to nearly 60 different tRNAs, depending on the organism. It must unfold base-paired secondary structures, as well as tertiary structures, such as pseudoknots, in the mRNAs. All this is done rapidly (~1–10 codons s^{-1}) with high fidelity. The ribosome plus its translation factors EF-Tu and EF-G constitute a marvelous machine that has great flexibility for its RNA reactants, but very high precision for the product protein it makes. A detailed mechanism will help in revealing when and why ribosomes make mistakes, such as frameshifting, incorporating the wrong amino acid, or prematurely terminating.

Mechanism of Elongation

The kinetics of elongation have been extensively studied by the Rodnina-Wintermeyer group using stopped-flow fluorescence and

quench flow methods (129–132). They have obtained values for many of the rate constants in the reaction that can be used to calculate the time dependence of each species. **Figure 6** shows the decrease in fraction of empty A-sites and increase in fraction of A-sites containing an aminoacyl $tRNA^{aa}$ as a function of time. Two intermediates of the reaction are also shown (EF·Tu·GTP·$tRNA^{aa}$ bound and GTP hydrolyzed to form bound EF-Tu·GDP·$tRNA^{aa}$ = I_1). Once the correct $tRNA^{aa}$ is accommodated in the A-site, peptide bond formation is fast and not rate limiting. Next, formation of the hybrid state occurs (discussed in the next section, Single-Molecule Translation), and translocation finishes one step of the cycle.

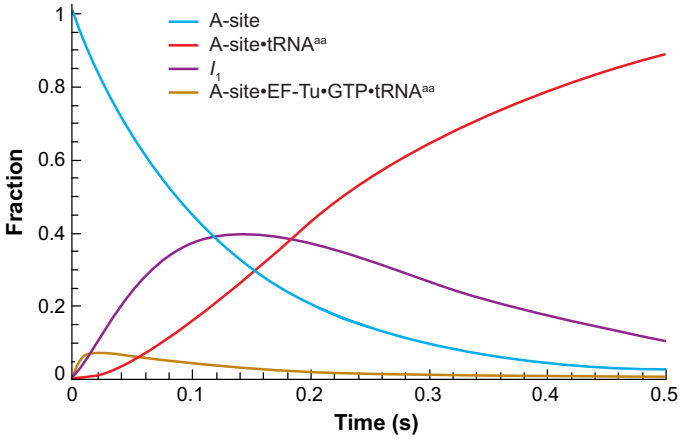

Figure 6

Time-dependence of the incorporation of a tRNA by EF-Tu into the A-site of a ribosome. The kinetic steps of the reaction are: A-site + EF − Tu·GTP·$tRNA^{aa}$ $\underset{k_{-1}}{\overset{k_1}{\rightleftarrows}}$ A-site·EF-Tu·GTP·$tRNA^{aa}$ $\xrightarrow{k_2}$ I_1 $\xrightarrow{k_3}$ A-site·$tRNA^{aa}$ + EF-Tu·GDP, I_1 = GTP hydrolyzed to form bound EF-Tu·GDP·$tRNA^{aa}$. The fraction of A-site reacted is calculated for $k_1 = 100\ \mu M^{-1}\ s^{-1}$; $k_{-1} = 25\ s^{-1}$; $k_2 = 35\ s^{-1}$; $k_3 = 7\ s^{-1}$ for a constant EF-Tu concentration of 0.1 μM. Data from Reference 129.

SINGLE-MOLECULE TRANSLATION

Figure 6 shows the fundamental limitation of ensemble kinetics; reactions occur asynchronously. This means that throughout the reaction reactants and products are both present, and intermediates will appear and disappear as the reaction proceeds. This mixture obviously complicates the problem of identifying and characterizing each species. In contrast, in single-molecule experiments there is only one species present at one time. When the reactant reacts, it is replaced by an intermediate, which is replaced by the next intermediate, which eventually is transformed to product. Instead of rate constants, the lifetime of each species is measured. The single-molecule reaction is repeated many times, each time yielding a different set of lifetimes for the species—because of the random nature of kinetics. The signal from two species in a stable equilibrium will exhibit "hopping" with the signal switching in time, and corresponding alternately to each state.

The distribution of lifetime values can reveal hidden intermediates between the measured species. For a reaction with N steps (N-1 intermediates) with equal rate constants, k, the distribution of lifetimes, τ, is a Poisson equation.

$$dP(\tau) = \left(\frac{k^N \tau^{N-1}}{(N-1)!}\right)(e^{-k\tau})d\tau \qquad 5.$$

Here $dP(\tau)/d\tau$ is the probability density of measuring a lifetime between τ and $\tau + d\tau$. If there are no intermediates ($N = 1$), the distribution is a simple exponential with a maximum at $\tau = 0$, and the mean value of the lifetimes, $\langle\tau\rangle = 1/k$. For any value of N, the distribution is at a maximum at $\tau = (N\text{-}1)/k$ with mean value $\langle\tau\rangle = N/k$. For hidden intermediates with unequal rate constants, the distribution will depend on differences of exponentials. Thus, any difference from an exponential distribution of lifetimes indicates hidden intermediates.

Blanchard et al. (133, 134) used FRET from fluorophore-labeled tRNAs to study the kinetics of tRNA selection and of translocation in single-molecule experiments. Prior to translocation, the tRNAs move to a hybrid state from the classical state (one tRNA is

in the P-site of both ribosomal subunits, and the other is in the A-site of both subunits). The process is a dynamic equilibrium with the classical state $tRNA^{peptide}$ in the A-site having a lifetime of 0.2 s. The hybrid state $tRNA^{peptide}$ shows two lifetimes with nearly equal probabilities for returning to the classical state (0.08 s, 0.39 s). These lifetimes (133) correspond to values of $k_{hybrid \rightarrow classic} = 5\ s^{-1}$ and $k_{classic \rightarrow hybrid} = 12.5\ s^{-1}$ and $2.5\ s^{-1}$. The ensemble results of the Rodnina-Wintermeyer group and the single-molecule results of the Puglisi-Chu group are consistent, which is encouraging. The review

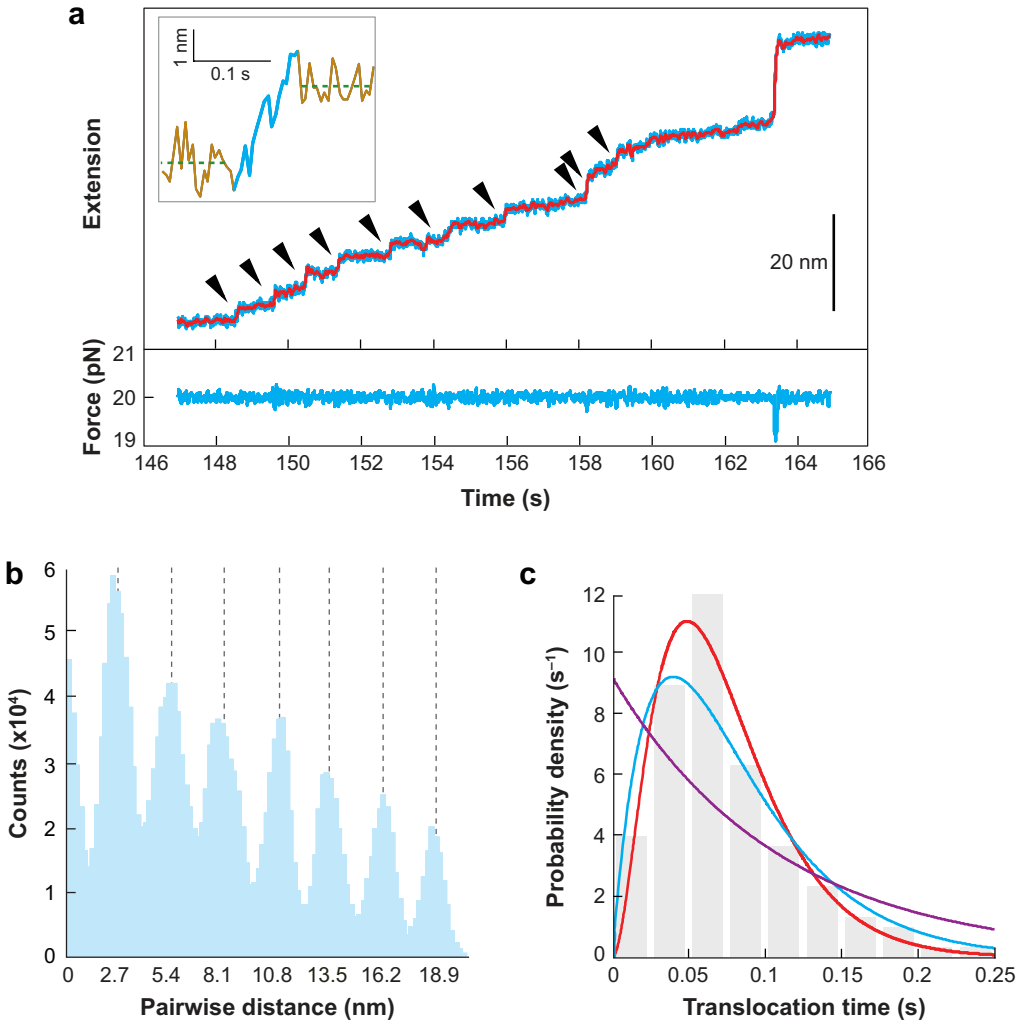

Figure 7

Single ribosome translation. (*a*) A trajectory of extension of mRNA versus time for the translation of an RNA hairpin by a single ribosome; an enlarged view of a single translocation step is shown as an inset. (*b*) Pairwise distribution of points showing that translocation occurs with steps of constant increase in extension of 2.7 nm, corresponding to translocation of 3 nts (1 codon) per step. (*c*) The distribution of translocation lifetimes fits a Poisson equation with three substeps corresponding to 23 ms per substep. The purple curve is the best fit to a one-substep reaction, blue is for two substeps, and red is for three substeps. Reprinted with permission from Reference 136.

by Puglisi et al. (135) in this volume gives much more details.

We (136) have measured the increase in extension of a single mRNA molecule as a ribosome translates the message. The method is identical to the one used in our single-molecule, laser tweezers studies of HCV NS3 RNA helicase (116). Beads are attached to the ends of a hairpin RNA and are held at a force below that necessary to unwind the hairpin. As the ribosome translates the 5′-side of the hairpin, the double helix is opened, releasing 1 nt on the 3′-side of the hairpin for each nucleotide translated. We thus measure a combination of the translocation and helicase activity of the ribosome. **Figure 7*a*** shows a time trace of the translation of a 60-bp hairpin containing only valine (GUN) and glutamic acid (GAPu) codons. Characteristic cycles of a long (1–2 s) pause followed by a short (0.1 s) translocation step are seen. The increase in end-to-end distance of the mRNA is 2.7 nm per step (**Figure 7*b***), which corresponds at 20-pN force to 6 nts unfolded per step. Thus at each step of translation, a codon of 3 nts is traversed by the ribosome, and another 3 nts are released from the duplex of the hairpin. The distribution of translocation lifetimes fits a Poisson equation with three identical substeps with mean lifetimes of 23 ms (**Figure 7*c***), corresponding to a mean translocation time of 69 ms. The measured mean translocation time was 78 ± 47 ms. The distribution of pause times indicates two substeps with different rate constants. Although the pause times can differ widely from ribosome to ribosome, and depend on the force applied to the RNA, the translocation times are independent of force and ribosome.

Single-molecule studies of translation are just beginning. The processes and states determined by FRET and by laser tweezers are not easily compared. During the pauses seen in the force experiments, the binding of EF-Tu, the recognition and insertion of the correct tRNA, and the binding of EF-G take place. Variation of concentrations of factors and substrates, and better time and distance resolution, are needed to identify and characterize each of the intermediates involved in one cycle of translation of one codon. In the FRET experiments, fluorophores placed on the ribosomal RNAs and proteins, the mRNA and the tRNAs can show relative motions of all the actors. Of course, ensemble studies will continue to provide important information. In a few years the goal of a step-by-step motion picture of the prokaryotic ribosome in action may be realized.

SUMMARY POINTS

1. Mechanical force can be applied to unfold single RNA molecules. Structural transitions, indicated by changes in the extension of the molecule, are monitored in real time. The free energy changes can be obtained from the mechanical work done to unfold the structure.
2. Single-molecule force manipulation can be used to control the structure and folding pathways of large RNAs, allowing characterization of sequential un/refolding steps. Force can also induce RNA misfolding.
3. Single-molecule fluorescence techniques are powerful in studying tertiary folding and domain dynamics of RNA structures, as well as in characterizing detailed reaction mechanisms of ribozymes.
4. Single-molecule force and fluorescence studies have elucidated the mechanisms by which helicases unwind DNA or RNA duplexes and convert chemical energy into mechanical work.

5. Translation by a single ribosome on a single RNA occurs by successive cycles of translocation steps and pauses. Each translocation step involves a motion of the RNA by 3 nts—one codon. Ribosome possesses helicase activity that can unwind secondary structures in mRNA during translation.

FUTURE ISSUES

1. Temperature-controlled optical tweezers should be applied to directly measure enthalpy and entropy changes of RNA folding at physiological temperatures. Kinetics of folding as a function of temperature are also needed.
2. More theoretical effort is needed to explain force unfolding kinetics, especially for intermediates and misfolded structures.
3. It remains unclear how RNA binding proteins, particularly chaperones, change the RNA structure. Assembly processes of large ribonucleoproteins, such as the spliceosome and telomere, are also not clear. Single-molecule techniques may solve some of these puzzles.
4. There are many different helicases and nucleic acid translocases. Single-molecule assays can provide detailed mechanisms for the activities of these molecular motors with different functions.
5. Single-ribosome translation assays can answer perennial questions on the effects of messenger RNA structure on translation. A single example is: What is the mechanism of pseudoknot-induced translational frameshifting?

DISCLOSURE STATEMENT

The authors are not aware of any biases that might be perceived as affecting the objectivity of this review.

ACKNOWLEDGMENTS

We thank our colleagues who provided high-resolution figures (**Figures 2, 3, 4–7**). This work was supported by National Institutes of Health grant GM-10840 (I.T.), a grant from University of Albany (P.T.X.L.), and a Graduate Research and Education in Adaptive bio-Technology (GREAT) Fellowship (J.V.).

LITERATURE CITED

1. Tinoco I Jr, Bustamante C. 1999. *J. Mol. Biol.* 293:271–81
2. Lu ZJ, Turner DH, Mathews DH. 2006. *Nucleic Acids Res.* 34:4912–24
3. Zuker M. 2003. *Nucleic Acids Res.* 31:3406–15
4. Hofacker IL. 2003. *Nucleic Acids Res.* 31:3429–31
5. Dirks RM, Bois JS, Schaeffer JM, Winfree E, Pierce NA. 2007. *SIAM Rev.* 49:65–88
6. Liphardt J, Onoa B, Smith SB, Tinoco I Jr, Bustamante C. 2001. *Science* 292:733–37
7. Mangeol P, Cote D, Bizebard T, Legrand O, Bockelmann U. 2006. *Eur. Phys. J. E Soft Matter* 19:311–17

8. Collin D, Ritort F, Jarzynski C, Smith SB, Tinoco I Jr, Bustamante C. 2005. *Nature* 437:231–34
9. Li PTX, Collin D, Smith SB, Bustamante C, Tinoco I Jr. 2006. *Biophys. J.* 90:250–60
10. Woodside MT, Anthony PC, Behnke-Parks WM, Larizadeh K, Herschlag D, Block SM. 2006. *Science* 314:1001–4
11. Woodside MT, Behnke-Parks WM, Larizadeh K, Travers K, Herschlag D, Block SM. 2006. *Proc. Natl. Acad. Sci. USA* 103:6190–95
12. Tinoco I Jr. 2004. *Annu. Rev. Biophys. Biomol. Struct.* 33:363–85
13. Seol Y, Skinner GM, Visscher K. 2004. *Phys. Rev. Lett.* 93:118102
14. Seol Y, Skinner GM, Visscher K, Buhot A, Halperin A. 2007. *Phys. Rev. Lett.* 98:158103
15. Green NH, Williams PM, Wahab O, Davies MC, Roberts CJ, et al. 2004. *Biophys. J.* 86:3811–21
16. Evans E, Ritchie K. 1997. *Biophys. J.* 72:1541–55
17. Jarzynski C. 1997. *Phys. Rev. Lett.* 78:2690–93
18. Crooks GE. 1999. *Phys. Rev. E* 60:2721–26
19. Liphardt J, Dumont S, Smith SB, Tinoco I Jr, Bustamante C. 2002. *Science* 296:1832–35
20. Hummer G, Szabo A. 2005. *Acc. Chem. Res.* 38:504–13
21. Minh DD. 2006. *Phys. Rev. E* 74:061120
22. Smith S, Cui Y, Bustamante C. 2003. *Methods Enzymol.* 361:134–62
23. Manosas M, Wen JD, Li PTX, Smith SB, Bustamante C, et al. 2007. *Biophys. J.* 92:3010–21
24. Wen JD, Manosas M, Li PTX, Smith SB, Bustamante C, et al. 2007. *Biophys. J.* 92:2996–3009
25. Gralla J, DeLisi C. 1974. *Nature* 248:330–32
26. Lindahl T, Adams A, Fresco JR. 1966. *Proc. Natl. Acad. Sci. USA* 55:941–48
27. Li PTX, Bustamante C, Tinoco I Jr. 2007. *Proc. Natl. Acad. Sci. USA* 104:7039–44
28. Hyeon C, Thirumalai D. 2005. *Proc. Natl. Acad. Sci. USA* 102:6789–94
29. Hyeon C, Thirumalai D. 2006. *Biophys. J.* 90:3410–27
30. Hyeon C, Thirumalai D. 2007. *Biophys. J.* 92:731–43
31. Manosas M, Ritort F. 2005. *Biophys. J.* 88:3224–42
32. Manosas M, Ritort F. 2006. *Phys. Rev. Lett.* 96:218301
33. Ha T, Zhuang X, Kim HD, Orr JW, Williamson JR, Chu S. 1999. *Proc. Natl. Acad. Sci. USA* 96:9077–82
34. Joo C, Balci H, Ishitsuka Y, Buranachai C, Ha T. 2008. *Annu. Rev. Biochem.* 77:51–76
35. Cate JH, Gooding AR, Podell E, Zhou K, Golden BL, et al. 1996. *Science* 273:1678–85
36. Jaeger L, Westhof E, Leontis NB. 2001. *Nucleic Acids Res.* 29:455–63
37. Hodak JH, Downey CD, Fiore JL, Pardi A, Nesbitt DJ. 2005. *Proc. Natl. Acad. Sci. USA* 102:10505–10
38. Downey CD, Fiore JL, Stoddard CD, Hodak JH, Nesbitt DJ, Pardi A. 2006. *Biochemistry* 45:3664–73
39. Bartley LE, Zhuang X, Das R, Chu S, Herschlag D. 2003. *J. Mol. Biol.* 328:1011–26
40. Latham JA, Cech TR. 1989. *Science* 245:276–82
41. Brunel C, Marquet R, Romby P, Ehresmann C. 2002. *Biochimie* 84:925–44
42. Li PTX, Bustamante C, Tinoco I Jr. 2006. *Proc. Natl. Acad. Sci. USA* 103:15847–52
43. Giedroc DP, Theimer CA, Nixon PL. 2000. *J. Mol. Biol.* 298:167–85
44. Theimer CA, Feigon J. 2006. *Curr. Opin. Struct. Biol.* 16:307–18
45. Shih IH, Been MD. 2002. *Annu. Rev. Biochem.* 71:887–917
46. Rivas E, Eddy SR. 1999. *J. Mol. Biol.* 285:2053–68

47. Isambert H, Siggia ED. 2000. *Proc. Natl. Acad. Sci. USA* 97:6515–20
48. Huang X, Ali H. 2007. *Nucleic Acids Res.* 35:656–63
49. Cao S, Chen SJ. 2007. *J. Mol. Biol.* 367:909–24
50. Hansen TM, Reihani SN, Oddershede LB, Sorensen MA. 2007. *Proc. Natl. Acad. Sci. USA* 104:5830–35
51. Green L, Kim CH, Bustamante C, Tinoco I Jr. 2008. *J. Mol. Biol.* 375:511–28
52. Shapiro BA, Yingling YG, Kasprzak W, Bindewald E. 2007. *Curr. Opin. Struct. Biol.* 17:157–65
53. Sotomayor M, Schulten K. 2007. *Science* 316:1144–48
54. Rhodes MM, Reblova K, Sponer J, Walter NG. 2006. *Proc. Natl. Acad. Sci. USA* 103:13380–85
55. Zhuang X, Bartley LE, Babcock HP, Russell R, Ha T, et al. 2000. *Science* 288:2048–51
56. Lilley DM. 2005. *Curr. Opin. Struct. Biol.* 15:313–23
57. Zhuang X. 2005. *Annu. Rev. Biophys. Biomol. Struct.* 34:399–414
58. Nahas MK, Wilson TJ, Hohng S, Javie K, Lilley DM, Ha T. 2004. *Nat. Struct. Mol. Biol.* 11:1107–13
59. Liu S, Bokinsky G, Walter NG, Zhuang X. 2007. *Proc. Natl. Acad. Sci. USA* 104:12634–39
60. Fiammengo R, Jäschke A. 2005. *Curr. Opin. Biotechnol.* 16:614–21
61. Gilbert W. 1986. *Nature* 319:618
62. Kobitski AY, Nierth A, Helm M, Jäschke A, Nienhaus GU. 2007. *Nucleic Acids Res.* 35:2047–59
63. Manning GS. 1969. *J. Chem. Phys.* 51:924–33
64. Magdelenat H, Turq P, Chemla M. 1974. *Biopolymers* 13:1535–48
65. Manning GS. 1979. *Accts. Chem. Res.* 12:443–49
66. De Rose VJ. 2003. *Curr. Opin. Struct. Biol.* 13:317–24
67. Draper DE, Grilley D, Soto AM. 2005. *Annu. Rev. Biophys. Biomol. Struct.* 34:221–43
68. Pyle AM, Fedorova O, Waldsich C. 2007. *Trends Biochem. Sci.* 32:138–45
69. Sharp KA, Honig B. 1995. *Curr. Opin. Struct. Biol.* 5:323–28
70. Woodson SA. 2005. *Curr. Opin. Chem. Biol.* 9:104–9
71. Sigel RK, Pyle AM. 2007. *Chem. Rev.* 107:97–113
72. Rueda D, Wick K, McDowell SE, Walter NG. 2003. *Biochemistry* 42:9924–36
73. Soto AM, Misra V, Draper DE. 2007. *Biochemistry* 46:2973–83
74. Anderson CF, Record MT Jr. 1995. *Annu. Rev. Phys. Chem.* 46:657–700
75. Tinoco I Jr, Li PTX, Bustamante C. 2006. *Q. Rev. Biophys.* 39:325–60
76. Record MT Jr, Anderson CF. 1993. *J. Phys. Chem.* 97:7116–26
77. Sharp KA, Friedman RA, Misra V, Hecht J, Honig B. 1995. *Biopolymers* 36:245–62
78. Zacharias M, Luty BA, Davis ME, McCammon JA. 1992. *Biophys. J.* 63:1280–85
79. Misra VK, Draper DE. 2001. *Proc. Natl. Acad. Sci. USA* 98:12456–61
80. Bloomfield VA, Crothers DM, Tinoco I Jr. 2000. See Ref. 137, pp. 475–534
81. Cantor CR, Schimmel PR. 1980. In *Biophysical Chemistry*, pp. 1109–77. New York: Freeman
82. Sun X, Zhang Q, Al-Hashimi HM. 2007. *Nucleic Acids Res.* 35:1698–713
83. Zhang Q, Sun X, Watt ED, Al-Hashimi HM. 2006. *Science* 311:653–56
84. Foloppe N, Matassova N, Aboul-Ela F. 2006. *Drug Discov. Today* 11:1019–27
85. Sucheck SJ, Wong CH. 2000. *Curr. Opin. Chem. Biol.* 4:678–86
86. Onoa B, Dumont S, Liphardt J, Smith SB, Tinoco I Jr, Bustamante C. 2003. *Science* 299:1892–95
87. Doherty EA, Doudna JA. 2000. *Annu. Rev. Biochem.* 69:597–615

88. Cochrane JC, Lipchock SV, Strobel SA. 2007. *Chem. Biol.* 14:97–105
89. Lorenz C, Piganeau N, Schroeder R. 2006. *Nucleic Acids Res.* 34:334–42
90. Weixlbaumer A, Werner A, Flamm C, Westhof E, Schroeder R. 2004. *Nucleic Acids Res.* 32:5126–33
91. McCauley MJ, Williams MC. 2007. *Biopolymers* 85:154–68
92. Vladescu ID, McCauley MJN, Nuñez ME, Rouzina I, Williams MC. 2007. *Nat. Methods* 4:517–22
93. Koch SJ, Shundrovsky A, Jantzen BC, Wang MD. 2002. *Biophys. J.* 83:1098–105
94. Koch SJ, Wang MD. 2003. *Phys. Rev. Lett.* 91:028103
95. Jiang J, Bai L, Surtees JA, Gemici Z, Wang MD, Alani E. 2005. *Mol. Cell* 20:771–81
96. Tinoco I Jr, Collin D, Li PTX. 2004. *Biochem. Soc. Trans.* 32:757–60
97. Bokinsky G, Zhuang X. 2005. *Acc. Chem. Res.* 38:566–73
98. Johnson JE, Chiu W. 2007. *Curr. Opin. Struct. Biol.* 17:237–43
99. Shu D, Zhang H, Jin J, Guo P. 2007. *EMBO J.* 26:527–37
100. Levin JG, Guo J, Rouzina I, Musier-Forsyth K. 2005. *Prog. Nucleic Acid Res. Mol. Biol.* 80:217–86
101. Liu HW, Zeng Y, Landes CF, Kim YJ, Zhu Y, et al. 2007. *Proc. Natl. Acad. Sci. USA* 104:5261–67
102. Zeng Y, Liu HW, Landes CF, Kim YJ, Ma X, et al. 2007. *Proc. Natl. Acad. Sci. USA* 104:12651–56
103. Stone MD, Mihalusova M, O'Connor CM, Prathapam R, Collins K, Zhuang X. 2007. *Nature* 446:458–61
104. Turner DH. 2000. See Ref. 137, pp. 259–334
105. Singleton MR, Dillingham MS, Wigley DB. 2007. *Annu. Rev. Biochem.* 76:23–50
106. Rocak S, Linder P. 2004. *Nat. Rev. Mol. Cell Biol.* 5:232–41
107. Kim JL, Morgenstern KA, Griffith JP, Dwyer MD, Thomson JA, et al. 1998. *Structure* 6:89–100
108. Rudolph MG, Heissmann R, Wittmann JG, Klostermeier D. 2006. *J. Mol. Biol.* 361:731–43
109. Delagoutte E, von Hippel PH. 2002. *Q. Rev. Biophys.* 35:431–78
110. Delagoutte E, von Hippel PH. 2003. *Q. Rev. Biophys.* 36:1–69
111. Rasnik I, Myong S, Ha T. 2006. *Nucleic Acids Res.* 34:4225–31
112. Jankowsky E, Gross CH, Shuman S, Pyle AM. 2000. *Nature* 403:447–51
113. Kawaoka J, Jankowsky E, Pyle AM. 2004. *Nat. Struct. Mol. Biol.* 11:526–30
114. Serebrov V, Pyle AM. 2004. *Nature* 430:476–80
115. Levin MK, Gurjar M, Patel SS. 2005. *Nat. Struct. Mol. Biol.* 12:429–35
116. Dumont S, Cheng W, Serebrov V, Beran RK, Tinoco I Jr, et al. 2006. *Nature* 439:105–8
117. Cheng W, Dumont S, Tinoco I Jr, Bustamante C. 2007. *Proc. Natl. Acad. Sci. USA* 104:13954–59
118. Lucius AL, Maluf NK, Fischer CJ, Lohman TM. 2003. *Biophys. J.* 85:2224–39
119. Myong S, Bruno MM, Pyle AM, Ha T. 2007. *Science* 317:513–16
120. Astumian RD, Hanggi P. 2002. *Physics Today* 55:33–39
121. Johnson DS, Bai L, Smith BY, Patel SS, Wang MD. 2007. *Cell* 129:1299–309
122. Ahlquist P. 2002. *Science* 296:1270–73
123. Landick R. 2006. *Biochem. Soc. Trans.* 34:1062–66
124. Steitz TA. 2006. *EMBO J.* 25:3458–68
125. Bai L, Santangelo TJ, Wang MD. 2006. *Annu. Rev. Biophys. Biomol. Struct.* 35:343–60

126. Galburt EA, Grill SW, Wiedmann A, Lubkowska L, Choy J, et al. 2007. *Nature* 446:820–23
127. Spirin AS. 2000. *Ribosomes*. New York: Springer. 422 pp.
128. Liljas A. 2004. *Structural Aspects of Protein Synthesis*. Singapore: World Sci.
129. Pape T, Wintermeyer W, Rodnina MV. 1998. *EMBO J.* 17:7490–97
130. Wilden B, Savelsbergh A, Rodnina MV, Wintermeyer W. 2006. *Proc. Natl. Acad. Sci. USA* 103:13670–75
131. Savelsbergh A, Katunin VI, Mohr D, Peske F, Rodnina MV, Wintermeyer W. 2003. *Mol. Cell.* 11:1517–23
132. Wintermeyer W, Peske F, Beringer M, Gromadski KB, Savelsbergh A, Rodnina MV. 2004. *Biochem. Soc. Trans* 32:733–37
133. Blanchard SC, Gonzalez RL, Kim HD, Chu S, Puglisi JD. 2004. *Nat. Struct. Mol. Biol.* 11:1008–14
134. Blanchard SC, Kim HD, Gonzalez RL Jr, Puglisi JD, Chu S. 2004. *Proc. Natl. Acad. Sci. USA* 101:12893–98
135. Marshall RA, Aitken CE, Dorywalska M, Puglisi JD. 2007. *Annu. Rev. Biochem.* 77:177–203
136. Wen J-D, Lancaster L, Hodges C, Zeri A-C, Yoshimura SH, et al. 2008. *Nature*. 452:598–603
137. Bloomfield VA, Crothers DM, Tinoco I Jr. 2000. *Nucleic Acids: Structure, Properties and Functions*. Sausalito, CA: Univ. Sci. Books

Annual Review of Biochemistry

Volume 77, 2008

Contents

Prefatory Chapters

Discovery of G Protein Signaling
Zvi Selinger 1

Moments of Discovery
Paul Berg 14

Single-Molecule Theme

In singulo Biochemistry: When Less Is More
Carlos Bustamante 45

Advances in Single-Molecule Fluorescence Methods for Molecular Biology
Chirlmin Joo, Hamza Balci, Yuji Ishitsuka, Chittanon Buranachai, and Taekjip Ha 51

How RNA Unfolds and Refolds
Pan T.X. Li, Jeffrey Vieregg, and Ignacio Tinoco, Jr. 77

Single-Molecule Studies of Protein Folding
Alessandro Borgia, Philip M. Williams, and Jane Clarke 101

Structure and Mechanics of Membrane Proteins
Andreas Engel and Hermann E. Gaub 127

Single-Molecule Studies of RNA Polymerase: Motoring Along
Kristina M. Herbert, William J. Greenleaf, and Steven M. Block 149

Translation at the Single-Molecule Level
R. Andrew Marshall, Colin Echeverría Aitken, Magdalena Dorywalska, and Joseph D. Puglisi 177

Recent Advances in Optical Tweezers
Jeffrey R. Moffitt, Yann R. Chemla, Steven B. Smith, and Carlos Bustamante 205

Recent Advances in Biochemistry

Mechanism of Eukaryotic Homologous Recombination
Joseph San Filippo, Patrick Sung, and Hannah Klein 229

Structural and Functional Relationships of the XPF/MUS81 Family of Proteins
Alberto Ciccia, Neil McDonald, and Stephen C. West 259

Fat and Beyond: The Diverse Biology of PPARγ
Peter Tontonoz and Bruce M. Spiegelman 289

Eukaryotic DNA Ligases: Structural and Functional Insights
Tom Ellenberger and Alan E. Tomkinson 313

Structure and Energetics of the Hydrogen-Bonded Backbone in Protein Folding
D. Wayne Bolen and George D. Rose 339

Macromolecular Modeling with Rosetta
Rhiju Das and David Baker 363

Activity-Based Protein Profiling: From Enzyme Chemistry to Proteomic Chemistry
Benjamin F. Cravatt, Aaron T. Wright, and John W. Kozarich 383

Analyzing Protein Interaction Networks Using Structural Information
Christina Kiel, Pedro Beltrao, and Luis Serrano 415

Integrating Diverse Data for Structure Determination of Macromolecular Assemblies
Frank Alber, Friedrich Förster, Dmitry Korkin, Maya Topf, and Andrej Sali 443

From the Determination of Complex Reaction Mechanisms to Systems Biology
John Ross 479

Biochemistry and Physiology of Mammalian Secreted Phospholipases A_2
Gérard Lambeau and Michael H. Gelb 495

Glycosyltransferases: Structures, Functions, and Mechanisms
L.L. Lairson, B. Henrissat, G.J. Davies, and S.G. Withers 521

Structural Biology of the Tumor Suppressor p53
Andreas C. Joerger and Alan R. Fersht 557

Toward a Biomechanical Understanding of Whole Bacterial Cells
Dylan M. Morris and Grant J. Jensen 583

How Does Synaptotagmin Trigger Neurotransmitter Release?
Edwin R. Chapman 615

Protein Translocation Across the Bacterial Cytoplasmic Membrane
Arnold J.M. Driessen and Nico Nouwen 643

Maturation of Iron-Sulfur Proteins in Eukaryotes: Mechanisms, Connected Processes, and Diseases
Roland Lill and Ulrich Mühlenhoff 669

CFTR Function and Prospects for Therapy
John R. Riordan 701

Aging and Survival: The Genetics of Life Span Extension by Dietary Restriction
William Mair and Andrew Dillin 727

Cellular Defenses against Superoxide and Hydrogen Peroxide
James A. Imlay 755

Toward a Control Theory Analysis of Aging
Michael P. Murphy and Linda Partridge 777

Indexes

Cumulative Index of Contributing Authors, Volumes 73–77 799

Cumulative Index of Chapter Titles, Volumes 73–77 803

Errata

An online log of corrections to *Annual Review of Biochemistry* articles may be found at http://biochem.annualreviews.org/errata.shtml